How to cite: *Angew. Chem. Int. Ed.* **2023**, *62*, e202307530
doi.org/10.1002/anie.202307530

VIP **Systems Chemistry** *Very Important Paper*

ATP Drives the Formation of a Catalytic Hydrazone through an Energy Ratchet Mechanism

*Tommaso Marchetti, Diego Frezzato, Luca Gabrielli, and Leonard J. Prins**

Abstract: An energy ratchet mechanism is exploited for the synthesis of a molecule. In the presence of adenosine triphosphate (ATP), hydrazone-bond formation between an aldehyde and hydrazide is accelerated and the composition at thermodynamic equilibrium is shifted towards the hydrazone. Enzymatic hydrolysis of ATP installs a kinetically stable state, at which hydrazone is present at a higher concentration compared to the composition at thermodynamic equilibrium in the presence of the degradation products of ATP. It is shown that the kinetic state has an enhanced catalytic activity in the hydrolysis of an RNA-model compound.

The development of synthetic matter endowed with life-like properties requires the ability to rationally design systems that operate away from thermodynamic equilibrium at the expense of energy.[1,2,3,4] Great strides have been made in the development of synthetic molecular machinery able to convert energy in the form of light, electricity, or chemicals into work.[5,6,7] Theoretical and experimental studies have revealed that energy and information ratchet mechanisms play an essential role in driving molecular devices to a non-equilibrium state characterized by directional motion or by the population of a kinetic state in a self-assembly process.[8,9,10,11] Dissipative materials have been developed that rely on energy input to maintain structural integrity and display emerging properties.[12,13,14,15] It has been postulated that non-equilibrium self-assembly relies on the same ratchet mechanisms that drive molecular machines.[16,17,18,19] Experimental observations such as catastrophic collapse in supramolecular fibers,[20] oscillations[21,22] and cooperative catalysis[23,24] in the assembled state indeed suggest that ratchet mechanisms are embedded in these systems. Yet, unequivocal proof for their presence is hampered by the complexity of these systems which complicates a detailed kinetic and thermodynamic analysis of all occurring processes.[17,25,26] For that reason we turned our attention to the study of simple systems that are well-defined at the molecular level (Figure 1). Previously, Lehn and co-workers have shown that macrocyclic imines with high-strain energy can be prepared through an energy ratchet mechanism.[27] The approach relied on metal-ion templated cyclization followed by thermodynamically driven demetallation to yield a kinetically stable macrocycle. Here, we show that an energy consumption process can be used to shift a reaction

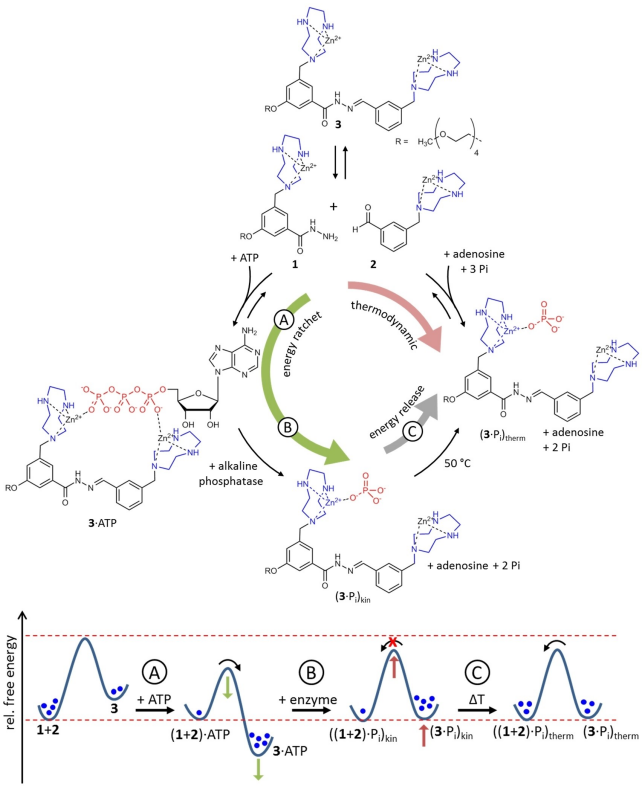

Figure 1. Equilibrium reaction between hydrazide **1**, aldehyde **2** and hydrazone **3**. The energy ratchet (green arrow) is composed of two steps: **A**—addition of ATP lowers the energy barrier for hydrazone formation and stabilizes the ground state of the product (**3**) more than that of the reactants (**1**+**2**), **B**—enzymatic hydrolysis of ATP reinstalls a high energy barrier for equilibration and eliminates the difference in ground-state energy. The kinetically stable mixture enriched in **3** can be converted into the equilibrium composition upon heating (step **C**). The same thermodynamically stable mixture can be obtained directly by equilibrating **1** and **2** in the presence of the phosphate mixture (A+3 P_i) (red arrow). Note that the chemical structure of the complex **3**·ATP is just a representation and that the energy diagrams represent the relative changes in free energy between the reactants and product of the equilibrium reaction.

[*] T. Marchetti, Dr. D. Frezzato, Dr. L. Gabrielli, Prof. Dr. L. J. Prins
Department of Chemical Sciences, University of Padua
Via Marzolo1, 35131 Padua (Italy)
E-mail: leonard.prins@unipd.it

away from the composition at equilibrium (Figure 1). The involved equilibrium reaction regards the formation of a hydrazone between an aldehyde and hydrazide. This reaction falls into the class of imine-type dynamic covalent bond formation, which is one of the most applied reactions for the development of supramolecular systems.[28,29,30,31] An energy ratchet mechanism is exploited in which in the first step a chemical trigger, ATP, is used to accelerate the reaction and to stabilize the hydrazone. In the second step, enzymatic degradation of ATP installs a kinetically stable state in which the hydrazone concentration is higher than the one at equilibrium. We show that the system in the non-equilibrium state has a higher catalytic activity in the hydrolysis of an RNA-model compound compared to the equilibrium state.

We synthesized hydrazide **1** and aldehyde **2**, which are both equipped with a 1,4,7-triazacyclononane (TACN)·Zn^{II}-complex (Figure 1). Hydrazone formation was studied by mixing **1** and **2** in an equimolar ratio (0.5 mM) in water buffered at pH 7.0 and monitoring changes in the ^{1}H NMR spectrum as a function of time at 25 °C (Figure 2a—blue trace and Figure 2b, Figure S2). Hydrazone formation was confirmed by a gradual decrease of the aldehyde signal at 9.91 ppm and a gradual increase of the signals at 8.39 and 8.67 ppm corresponding to the *E*- and *Z*-isomers of hydrazone **3**, respectively (Figure 2b-II and Figure S1).[32] However, hydrazone formation was extraordinary slow ($k_{f,3} = 4.8 \pm 0.7 \times 10^{-2}$ M^{-1} min^{-1}) and even after 2 weeks at 25 °C equilibrium had not yet been reached. Carrying out the reaction at higher concentrations resulted in higher rates

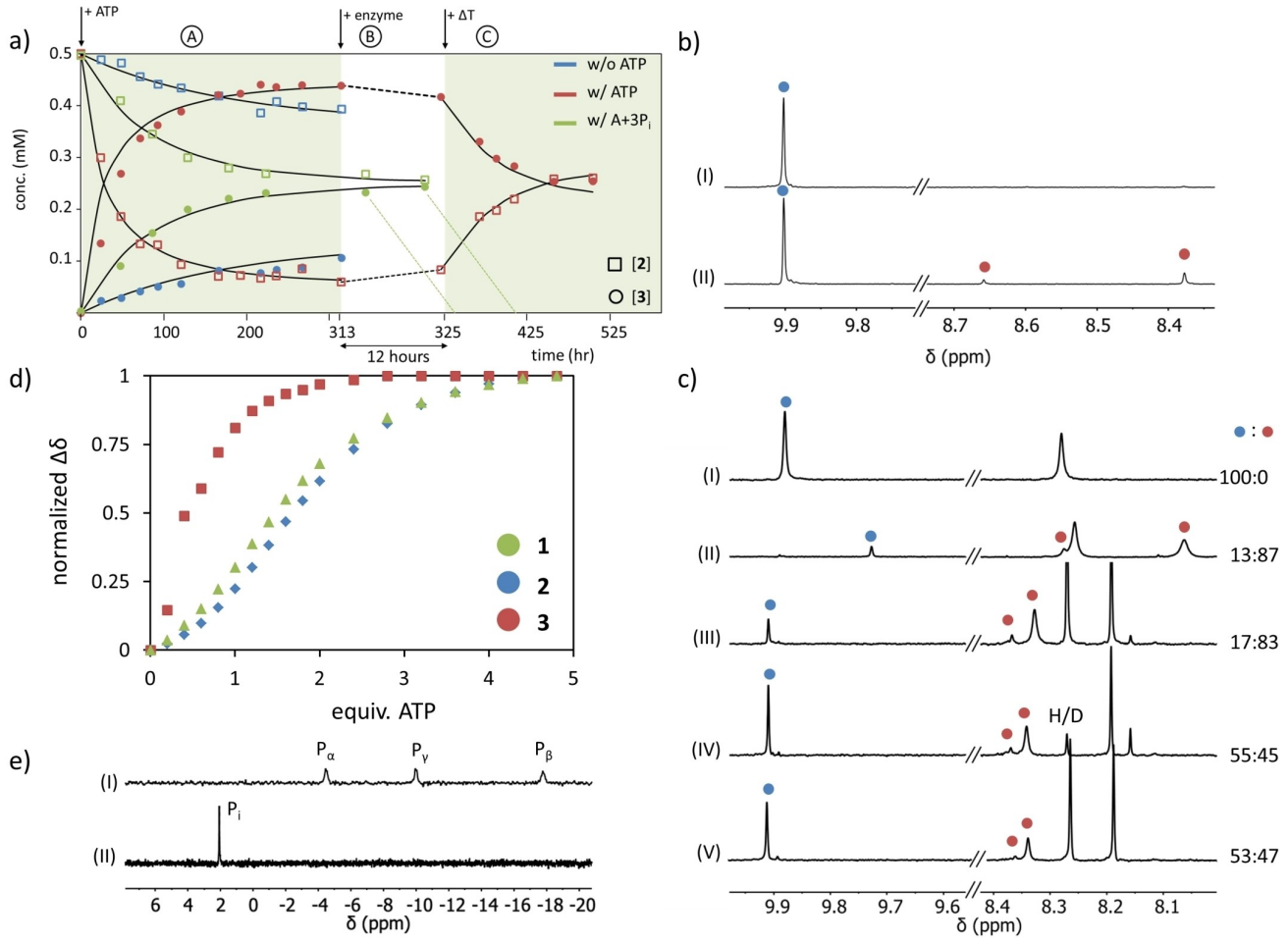

Figure 2. a) Changes in concentrations over time as determined by ^{1}H NMR spectroscopy (squares: aldehyde **2**, circles: hydrazone **3**). Symbols A–C refer to the events shown in Figure 1. In section A, formation of hydrazone **3** is reported for mixing **1** and **2** (blue trace), mixing **1** and **2** in the presence of ATP (red trace) and mixing **1** and **2** in the presence of the phosphate mixture (adenosine + 3 P_i, green trace). At t = 313 h, the enzyme alkaline phosphatase was added to the sample containing ATP (section B). After 12 h the sample was heated to 50 °C for equilibration (section C). b) Parts of the ^{1}H NMR spectra containing characteristic signals for **2** and **3** of a 1:1 mixture of **1** and **2** (at 0.5 mM each) corresponding to the blue trace in Figure 2a at t = 0 h (I) and t = 313 h (II). c) Parts of the ^{1}H NMR spectra containing characteristic signals for **2** and **3** at various stages of the kinetics reported in Figure 2a (red trace): t = 0 h (I), t = 313 h (II), t = 325 h (III—12 hours after addition of the enzyme), t = 510 h (IV—180 h after heating the sample at 50 °C). Figure 2c-V reports parts of the ^{1}H NMR spectrum of a mixture containing **1** and **2** at 0.5 mM each equilibrated in the presence of the phosphate mixture at 25 °C. d) Change in the chemical shift (normalized) of signals of **1**, **2**, and **3** upon the addition of ATP to a 1:1:1 mixture of **1**, **2**, and **3** (0.5 mM each). e) Parts of the ^{31}P NMR spectrum of the reaction mixture before (I) and 12 h after (II) the addition of enzyme.

and an equilibrium constant for the reaction could be determined ($K = 1.7 \times 10^3\ M^{-1}$, Figure S3). This value corresponds to an equilibrium composition at which hydrazone **3** is present for 35 % for $[\mathbf{1}]_0 = [\mathbf{2}]_0 = 0.5$ mM. Reactivity studies using structurally related hydrazides and aldehydes but lacking the TACN·Zn^{II}-complex revealed that the particularly slow reaction rate is related to the presence of the TACN·Zn^{II}-complexes (Figure S17). The presence of just one TACN·Zn^{II}-complex led to a 2- or 3-fold increase in rate of formation depending on whether the TACN·Zn^{II}-complex was present on the aldehyde or hydrazide. A 5-fold increase in rate was observed when neither one of the components contained a TACN·Zn^{II}-complex. Based on these observations, we hypothesized that the negative effect of the TACN·Zn^{II}-complexes on the rate of hydrazone-formation could possibly originate from their positive charge. If so, we argued that this effect could potentially be mitigated by adding adenosine triphosphate (ATP) as a strongly coordinating counter-anion for TACN·Zn^{II}.[33] NMR binding studies between ATP and either **1** or **2** (0.5 mM) showed that both compounds have a very high affinity for ATP ($K_{\mathbf{1}} > 10^5\ M^{-1}$; $K_{\mathbf{2}} = 1.1(\pm 0.1) \times 10^4\ M^{-1}$) (Supporting Information—section 2.11). This implies that complexes **1**·ATP and **2**·ATP are practically quantitatively formed in the presence of 1 equivalent of ATP. Hydrazone-bond formation between **1** and **2** was then repeated using an equimolar mixture of **1**, **2** and ATP (0.5 mM each) implying that sufficient ATP was present to bind half of the available TACN·Zn^{II}-complexes (Figure S5). An impressive 23-fold increase in the rate of formation of **3** was observed ($k_{f,\mathbf{3},\mathbf{ATP}} = 1.2 \pm 0.1\ M^{-1}min^{-1}$) (Figure 2a—red trace). Importantly, the presence of ATP not only affected the reaction kinetics, but also caused a shift in the equilibrium composition towards hydrazone **3**. At equilibrium, hydrazone **3** now accounted for 87 % instead of the 35 % calculated in the absence of ATP ($K_{ATP} = 1.4 \times 10^5\ M^{-1}$, with standard reaction free energy $\Delta G^{\ominus} = -29.3\ kJ.mol^{-1}$, Figure 2c-II). The effect of ATP on the equilibrium composition was confirmed in an independent experiment in which 1 equivalent of ATP was added to a pre-equilibrated mixture of **1**, **2** and **3** (Figure S10). The shift in the equilibrium composition suggested that the intrinsic stability of the **3**·ATP complex is likely the most important feature to explain the shift in composition. The higher stability of **3**·ATP was indeed confirmed by an NMR titration experiment in which increasing amounts of ATP were added to an equimolar mixture of **1**, **2** and **3** (each at 0.5 mM). The titration was conducted on a timescale at which the condensation reaction does not take place. Up to 0.5 mM of ATP—that is, 1 equivalent compared to the available TACN·Zn^{II} complexes—shifts in the ^{1}H NMR spectrum were mainly observed for **3** (Figure 2d and Figure S33). Signals of **1** and **2** started to shift significantly only when larger amounts of ATP were added (Figure 2d). In an alternative experiment, increasing amounts of a 1:1 mixture of **1** and **2** were added to complex **3**·ATP (0.5 mM) and changes in the ^{1}H NMR spectrum were monitored (Figure S31). Treating **1** and **2** as a fictitious species (**1**/**2**) yielded an apparent equilibrium constant of 6.7×10^{-2} between **3**·ATP and (**1**/**2**)·ATP indicating again a much higher affinity of ATP for **3** compared to the reactants. In summary, the reaction kinetics and binding studies show that ATP stabilizes both the transition state of the equilibrium reaction between **1**+**2** and **3** and the ground state of the product (**3**) compared to the reactants (**1**+**2**) (Figure 1). The strong interaction between **3** and ATP does not come as a surprise considering that it is well-known that ATP has a high affinity for multivalent systems decorated with multiple TACN·Zn^{II} complexes.[34,35] To study to which extent multivalency plays a role in this system we studied the effect on the equilibrium reaction of a mixture composed of 3 equivalents of inorganic phosphate, P_i, and 1 equivalent of adenosine. The choice for this particular mixture was not coincidental because it can be chemically derived from ATP upon treatment with the enzyme alkaline phosphatase.[36] We observed that also this phosphate mixture—at the concentration at which it would be obtained from 0.5 mM ATP—had a positive effect on both the reaction kinetics and thermodynamics, but to a much lesser extent compared to ATP (Figure 2a—green trace, Figure S7). A rate acceleration of just 4-fold was observed ($k_{f,Pi} = 0.21\ M^{-1}\ min^{-1}$) and at equilibrium hydrazone **3** accounted for just 47 % ($K_{Pi} = 3.9 \times 10^3\ M^{-1}$) (Figure 2a—green trace and Figure 2c-V). Thus, compared to ATP, the phosphate mixture stabilizes the transition state to a lower extent and has a much lower capacity to shift the equilibrium towards **3** (Figure 1).

The energy landscape corresponding to the phosphate mixture can be accessed from the ATP energy landscape by treating the ATP-system with the enzyme alkaline phosphatase.[37,38] Starting from the equilibrium mixture with ATP (**3** at 87 %), we added 100 $U.ml^{-1}$ of the enzyme alkaline phosphatase and confirmed with ^{31}P NMR that after 12 hours ATP had been completely converted into the phosphate mixture (Figure 2e). Importantly, during this period ^{1}H NMR showed only a minor change in the concentration of hydrazone **3** which still accounted for 83 % (Figure 2a—area B, Figure 2c—III and Figures S14 and S15). This implies that after ATP hydrolysis the system resided in a kinetically stable state enriched in hydrazone **3** ($\mathbf{3}_{kin} = 83$ %, $\mathbf{3}_{therm} = 47$ %). The population of this state is possible because the rate of ATP hydrolysis is higher than the rate of hydrazone hydrolysis. Evidence for the presence of a kinetically stable state came from the observation that heating the sample to 50 °C caused a gradual decrease in the concentration of **3** (Figure 2a—area C) eventually reaching the concentration (Figure 2c-IV) corresponding to the one observed at equilibrium in the presence of the phosphate mixture (Figure 2c-V and Figure S16). We verified that heating did not significantly shift the equilibrium composition in the presence of the phosphate mixture (Figure S8).

In the kinetically stable non-equilibrium state, the system owns an amount of "stored" Gibbs free energy which can be potentially exploited to perform work during the relaxation to equilibrium at constant pressure and temperature. In the limit of dilute solutions, the stored free energy per unit of volume can be computed as shown in section 4 of the Supporting Information. The resulting expression corresponds to the one used by Credi and co-workers to

determine the free energy density stored in the self-assembly steps of a supramolecular pump at the non-equilibrium steady state.[39] It is noted that the system studied in that work differs from the present one because here solvent participates in the reaction. With the concentrations at equilibrium and in the kinetically stable state, we estimate a stored free energy of 0.49 J/L.

Shifting a system towards a non-equilibrium composition becomes attractive when this leads to an enhancement of function.[40] Considering the well-known enhanced catalytic activity of clusters of TACN·Zn^{II}-complexes[41,42] in the transphosphorylation of 2-hydroxypropyl *p*-nitrophenyl-phosphate (HPNPP)—a model compound used for studying RNA hydrolysis—we studied the catalytic activity of the TACN·Zn^{II}-containing molecules **1**, **2** and **3** at the various stages of the process (Figure 3a and Supporting Information Section 3). First of all, we verified that hydrazone-formation led to an increase in catalytic activity. Hydrazone **3** converted HPNPP (2 mM) into cyclic phosphate and *p*-nitrophenol with an initial rate of 2.20×10^{-9} M.min^{-1} (Figure 3b - red trace) which is indeed 1.78-fold higher than the rate observed for a mixture of **1** and **2** at the same concentration of TACN·Zn^{II} (Figure 3b—blue trace). Although not large, the difference in activity is significant and sufficient enough to verify whether population of the kinetic state through the energy ratchet provides a means to enhance catalytic activity. As shown above, ATP-templated hydrazone formation leads to a mixture strongly enriched in **3**. This mixture is catalytically inactive because ATP is a strong inhibitor and blocks access of HPNPP to the catalytic site (Figure 3b—grey trace). Enzymatic hydrolysis of ATP in this mixture produces the kinetically stable state with an enhanced concentration of hydrazone **3**. This mixture is catalytically active because of the lower affinity of the phosphate mixture for **3** and an initial rate of 1.98×10^{-9} M.min^{-1} was determined (Figure 3b—green trace). This value is a bit lower than the rate observed for pure hydrazone **3** because of the presence of the weak phosphate inhibitors. Importantly though, the measured activity is higher than the activity measured for the identical mixture at thermodynamic equilibrium ($v_{init}=1.72\times10^{-9}$ M.min^{-1}, Figure 3b—purple trace). The p-value of 0.048 calculated using the Student's t-test shows that the difference is statistically significant (Supporting Information—Section 3). Compelling evidence for the enhanced activity of the system at the kinetic state was obtained by showing that conversion to the thermodynamic composition by heating at 50 °C for 180 hours caused a reduction of the catalytic activity ($v_{init}=1.74\times10^{-9}$ M.min^{-1}) corresponding to that of the mixture at thermodynamic equilibrium (Figure 3b—orange trace).

In conclusion, we have used an energy ratchet mechanism to drive a dynamic covalent reaction away from equilibrium. The addition of ATP both accelerates the reaction and stabilizes the product. The successive enzymatic degradation of ATP reinstalls high energy barriers for the equilibrium reaction and reduces the ground state stabilization of the product. Consequently, it brings the system into a kinetically stable state with a higher concentration of hydrazone compared to that at equilibrium. Exploiting ratchet mechanisms for the synthesis of molecules will be important for obtaining an understanding at the molecular level of how energy stored in kinetically stable, but thermodynamically activated molecules,[43] such as ATP, can be exploited to drive structure formation. Such detailed information is hard, if not impossible, to obtain for multivalent systems. From a practical point of view, the reported system displays evidently very slow reaction kinetics. We are well aware that imine-type bond formation can be accelerated using catalysts,[44] but here we have avoided their use to keep the number of interacting species as small as possible. In general, the use of energy ratchet mechanisms for dynamic covalent bond formation appears to be an attractive strategy for the development of new classes of supramolecular materials, catalysts, and sensors, that do not reside at thermodynamic equilibrium.

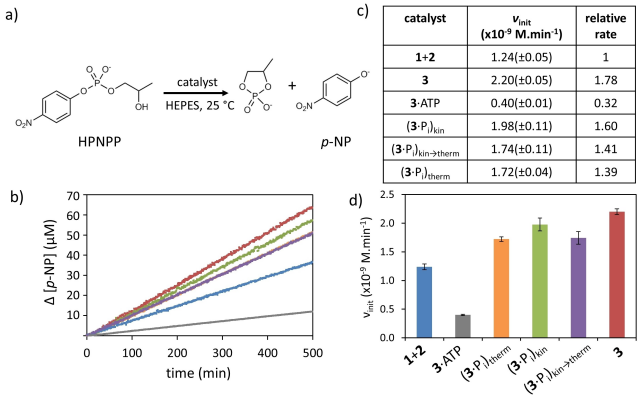

catalyst	v_{init} (x10^{-9} M.min^{-1})	relative rate
1+2	1.24(±0.05)	1
3	2.20(±0.05)	1.78
3·ATP	0.40(±0.01)	0.32
(3·P$_i$)$_{kin}$	1.98(±0.11)	1.60
(3·P$_i$)$_{kin→therm}$	1.74(±0.11)	1.41
(3·P$_i$)$_{therm}$	1.72(±0.04)	1.39

Figure 3. a) Catalysed transphosphorylation of HPNPP. b) Change in the concentration of *p*-NP as a function of time for different catalyst mixtures. Each measurement was carried out in triplicate; the average value is provided. The color codes correspond to those used in the histogram reported in Figure 3d. c) Absolute and relative initial rates for the different catalyst mixtures. d) Histogram containing the initial reaction rates for the different catalyst mixtures.

Supporting Information

The authors have cited additional references within the Supporting Information.[45–50]

Acknowledgements

This work was financially supported by the Italian Ministry of Education and Research (L.J.P., grant 2017E44A9P) and the University of Padova (L.J.P., grant P-DiSC #CASA-BIRD2022-UNIPD, and L.G. grant STARS-StG DyNA-seq).

Conflict of Interest

The authors declare no conflict of interest.

Data Availability Statement

The data that support the findings of this study are available from the corresponding author upon reasonable request.

Keywords: Dynamic Covalent Chemistry · Energy Ratchet · Non-Equilibrium · Supramolecular Catalysis · Systems Chemistry

[1] C. Cheng, P. R. McGonigal, J. F. Stoddart, R. D. Astumian, *ACS Nano* **2015**, *9*, 8672–8688.
[2] B. A. Grzybowski, W. T. S. Huck, *Nat. Nanotechnol.* **2016**, *11*, 585–592.
[3] A. Walther, *Adv. Mater.* **2020**, *32*, 1905111.
[4] G. Ashkenasy, T. M. Hermans, S. Otto, A. F. Taylor, *Chem. Soc. Rev.* **2017**, *46*, 2543–2554.
[5] S. Kassem, T. Van Leeuwen, A. S. Lubbe, M. R. Wilson, B. L. Feringa, D. A. Leigh, *Chem. Soc. Rev.* **2017**, *46*, 2592–2621.
[6] I. Aprahamian, *ACS Cent. Sci.* **2020**, *6*, 347–358.
[7] Y. Feng, M. Ovalle, J. S. W. Seale, C. K. Lee, D. J. Kim, R. D. Astumian, J. F. Stoddart, *J. Am. Chem. Soc.* **2021**, *143*, 5569–5591.
[8] E. R. Kay, D. A. Leigh, F. Zerbetto, *Angew. Chem. Int. Ed.* **2007**, *46*, 72–191.
[9] R. D. Astumian, C. Pezzato, Y. Feng, Y. Qiu, P. R. McGonigal, C. Cheng, J. F. Stoddart, *Mater. Chem. Front.* **2020**, *4*, 1304–1314.
[10] R. D. Astumian, *Acc. Chem. Res.* **2018**, *51*, 2653–2661.
[11] S. Amano, M. Esposito, E. Kreidt, D. A. Leigh, E. Penocchio, B. M. W. Roberts, *Nat. Chem.* **2022**, *14*, 530–537.
[12] S. A. P. Van Rossum, M. Tena-Solsona, J. H. Van Esch, R. Eelkema, J. Boekhoven, *Chem. Soc. Rev.* **2017**, *46*, 5519–5535.
[13] B. Rieß, R. K. Grötsch, J. Boekhoven, *Chem* **2020**, *6*, 552–578.
[14] R. Merindol, A. Walther, *Chem. Soc. Rev.* **2017**, *46*, 5588–5619.
[15] A. Mishra, S. Dhiman, S. J. George, *Angew. Chem. Int. Ed.* **2021**, *60*, 2740–2756.
[16] G. Ragazzon, L. J. Prins, *Nat. Nanotechnol.* **2018**, *13*, 882–889.
[17] K. Das, L. Gabrielli, L. J. Prins, *Angew. Chem. Int. Ed.* **2021**, *60*, 20120–20143.
[18] S. Amano, S. Borsley, D. A. Leigh, Z. Sun, *Nat. Nanotechnol.* **2021**, *16*, 1057–1067.
[19] E. Penocchio, G. Ragazzon, *Small* **2023**, *19*, 2206188.
[20] J. Boekhoven, W. E. Hendriksen, G. J. M. Koper, R. Eelkema, J. H. van Esch, *Science* **2015**, *349*, 1075–1079.
[21] J. Leira-Iglesias, A. Tassoni, T. Adachi, M. Stich, T. M. Hermans, *Nat. Nanotechnol.* **2018**, *13*, 1021–1027.
[22] M. G. Howlett, A. H. J. Engwerda, R. J. H. Scanes, S. P. Fletcher, *Nat. Chem.* **2022**, *14*, 805–810.
[23] P. Solís Muñana, G. Ragazzon, J. Dupont, C. Z. J. Ren, L. J. Prins, J. L. Y. Chen, *Angew. Chem. Int. Ed.* **2018**, *57*, 16469–16474.
[24] S. Bal, K. Das, S. Ahmed, D. Das, *Angew. Chem. Int. Ed.* **2019**, *58*, 244–247.
[25] A. Sharko, D. Livitz, S. De Piccoli, K. J. M. Bishop, T. M. Hermans, *Chem. Rev.* **2022**, *122*, 11759–11777.
[26] I. Aprahamian, S. M. Goldup, *J. Am. Chem. Soc.* **2023**, https://doi.org/10.1021/jacs.2c12665.
[27] L. Ratjen, G. Vantomme, J.-M. Lehn, *Chem. Eur. J.* **2015**, *21*, 10070–10081.
[28] M. E. Belowich, J. F. Stoddart, *Chem. Soc. Rev.* **2012**, *41*, 2003–2024.
[29] X. Su, I. Aprahamian, *Chem. Soc. Rev.* **2014**, *43*, 1963–1981.
[30] Y. Jin, Q. Wang, P. Taynton, W. Zhang, *Acc. Chem. Res.* **2014**, *47*, 1575–1586.
[31] J. R. Nitschke, *Acc. Chem. Res.* **2007**, *40*, 103–112.
[32] D. J. Van Dijken, P. Kovaříček, S. P. Ihrig, S. Hecht, *J. Am. Chem. Soc.* **2015**, *137*, 14982–14991.
[33] E. Rossi, A. Ferrarini, M. Sulpizi, *Phys. Chem. Chem. Phys.* **2023**, *25*, 6102–6111.
[34] C. Pezzato, L. J. Prins, *Nat. Commun.* **2015**, *6*, 7790.
[35] S. Maiti, I. Fortunati, C. Ferrante, P. Scrimin, L. J. Prins, *Nat. Chem.* **2016**, *8*, 725–731.
[36] D. Barford, A. K. Das, M. P. Egloff, *Annu. Rev. Biophys. Biomol. Struct.* **1998**, *27*, 133–164.
[37] M. Kumar, P. Brocorens, C. Tonnelé, D. Beljonne, M. Surin, S. J. George, *Nat. Commun.* **2014**, *5*, 5793.
[38] A. Sorrenti, J. Leira-Iglesias, A. Sato, T. M. Hermans, *Nat. Commun.* **2017**, *8*, 15899.
[39] S. Corra, M. Tranfić Bakić, J. Groppi, M. Baroncini, S. Silvi, E. Penocchio, M. Esposito, A. Credi, *Nat. Nanotechnol.* **2022**, *17*, 746–751.
[40] R. Chen, S. Neri, L. J. Prins, *Nat. Nanotechnol.* **2020**, *15*, 868–874.
[41] F. Manea, F. B. Houillon, L. Pasquato, P. Scrimin, *Angew. Chem. Int. Ed.* **2004**, *43*, 6165–6169.
[42] F. Mancin, L. J. Prins, P. Pengo, L. Pasquato, P. Tecilla, P. Scrimin, *Molecules* **2016**, *21*, 1014.
[43] C. T. Walsh, B. P. Tu, Y. Tang, *Chem. Rev.* **2018**, *118*, 1460–1494.
[44] D. K. Kölmel, E. T. Kool, *Chem. Rev.* **2017**, *117*, 10358–10376.
[45] T.-L. Hwang, A. J. Shaka, *J. Magn. Reson. Ser. A* **1995**, *112*, 275–279.
[46] L. Brunsveld, H. Zhang, M. Glasbeek, J. A. J. M. Vekemans, E. W. Meijer, *J. Am. Chem. Soc.* **2000**, *122*, 6175–6182.
[47] T. W. Kim, *Org. Lett.* **2005**, *7*, 111–114.
[48] G. Pieters, A. Cazzolaro, R. Bonomi, L. J. Prins, *Chem. Commun.* **2012**, *48*, 1916–1918.
[49] H. Zhang, F. Xie, M. Cheng, F. Peng, *J. Med. Chem.* **2019**, *62*, 6985–6991.
[50] J. M. Poolman, C. Maity, J. Boekhoven, L. Van der Mee, V. A. A. Le Sage, G. J. M. Groenewold, S. I. Van Kasteren, F. Versluis, J. H. Van Esch, R. Eelkema, *J. Mater. Chem. B* **2016**, *4*, 852–858.

Manuscript received: May 29, 2023
Accepted manuscript online: June 27, 2023
Version of record online: July 10, 2023